Int. J. Heat Mass Transfer. Vol. 36, No. 15, pp. 3723–3730, 1993
Printed in Great Britain

0017–9310/93 $6.00 + 0.00

Reynolds number effect on leading edge film effectiveness and heat transfer coefficient

ANANT B. MEHENDALE and JE-CHIN HAN
Turbine Heat Transfer Laboratory, Department of Mechanical Engineering,
Texas A&M University, College Station, TX 77843-3123, U.S.A.

(*Received* 19 *November* 1992 *and in final form* 5 *March* 1993)

Abstract—The effect of mainstream Reynolds number on leading edge heat transfer coefficient, film effectiveness, and heat flux was experimentally studied. Data were obtained for several combinations of film hole shapes and spacings, film hole row locations, blowing ratios, and mainstream turbulence levels at the Reynolds numbers of 100 000, 40 000, and 25 000. Representative results from 3-*d* and 4-*d* spaced two row injections, at the intermediate blowing ratio of 0.8, with and without turbulence grid are presented. Both heat transfer coefficient and film effectiveness increase with Reynolds number. A Reynolds number of 100 000 produces the lowest heat flux ratio in most of the leading edge region.

INTRODUCTION

THERE have been many investigations to study the effect of film injection on flat or slightly curved surfaces for low mainstream turbulence intensities. The effects of various blowing ratios, injection geometries, and film coolants have been investigated by Goldstein *et al.* [1, 2], Eriksen and Goldstein [3], Muska *et al.* [4], Sasaki *et al.* [5], Bergeles *et al.* [6], Mayle *et al.* [7], Jabbari and Goldstein [8], and Han and Mehendale [9]. Schönung and Rodi [10] developed a two-dimensional boundary layer procedure to calculate film cooling parameters for film injection over a flat plate. Mick and Mayle [11] studied the effect of leading edge film injection for a low mainstream turbulence flow on a leading edge model.

A leading edge model similar to that by Mick and Mayle [11] was used by the present researchers to study the effects of high mainstream turbulence, film hole shape, film hole spacing, film hole row location, and Reynolds number on film effectiveness and heat transfer coefficient. Mehendale *et al.* [12] studied the effect of high mainstream turbulence on leading edge heat transfer coefficients without film holes and found that an increase in mainstream turbulence causes an increase in heat transfer. They correlated the leading edge heat transfer coefficient ($Nu_D/Re_D^{0.5}$) with $Tu(Re_D)^{0.5}$. Mehendale and Han [13] studied the effect of high mainstream turbulence on leading edge film injection through two rows of film holes (3-*d* spacing) at $\pm 15°$ and $\pm 40°$. Ou *et al.* [14] studied the effects of high mainstream turbulence and film hole row location for film injection through a single row of film holes (3-*d* spacing) at $\pm 15°$ or $\pm 40°$. Ou and Han [15] studied the effect of high mainstream turbulence on film injection through two rows of film slots (3-*l* spacing) at $\pm 15°$ and $\pm 40°$. Mehendale and Han [16] studied the effects of high mainstream turbulence and film hole spacing (3-*d* and 4-*d*) for film injection through two rows of film holes at $\pm 15°$ and $\pm 40°$.

Apart from heat transfer coefficient and film effectiveness, another important parameter is heat flux ratio. It is the ratio of heat flux with film injection to heat flux without film holes, at the same test conditions. Thus, by definition, a heat flux ratio of less than unity indicates that film injection reduces heat transfer over the no film holes condition. In general, results from all these tests [13–16] indicate that: as the blowing ratio increases, the heat transfer coefficients on the leading edge increase; the blowing ratio of 0.4 provides the best film effectiveness for 3-*d* spacing, whereas, the blowing ratio of 0.8 provides the best film effectiveness for 4-*d* spacing and 3-*l* spacing; as the mainstream turbulence increases, the heat transfer coefficients on the leading edge increase, but the increases due to mainstream turbulence are reduced at higher blowing ratios; an increase in mainstream turbulence causes a reduction in film effectiveness, but the decreases due to mainstream turbulence are reduced at higher blowing ratios; the decreases in film effectiveness due to mainstream turbulence are most prominent at the blowing ratio of 0.4 for all film hole configurations studied; 4-*d* hole injection produces lower heat transfer coefficient and film effectiveness values than 3-*d* hole injection; 3-*l* slot injection produces lower heat transfer coefficients than 4-*d* hole injection; for the cases of single row film injection, the effect of mainstream turbulence is more prominent for $\pm 15°$ injection than $\pm 40°$ injection; heat flux ratios of less than unity are achieved at almost all locations under high mainstream turbulence conditions; the blowing ratio of 0.4 provides the lowest heat flux ratio for 3-*d* film injection, whereas, the blowing ratio of 0.8 provides the lowest heat flux ratio for 4-*d* and 3-*l* film injections; 3-*d* film injection provides lower heat flux ratio than 4-*d* film

NOMENCLATURE

d	film hole diameter	q''_{rad}	local radiation heat loss flux
D	leading edge diameter	$\overline{q''_0}$	spanwise averaged forced convection heat flux for the no film holes test model
h	local forced convection heat transfer coefficient with film injection	Re_D	Reynolds number based on the leading edge diameter
h_0	local forced convection heat transfer coefficient for the no film holes case	T_∞	ambient mainstream temperature
k	local thermal conductivity at film temperature	Tu	streamwise turbulence intensity
L	film hole length	U_s	average injectant velocity
$\dot{m}_{15}$	mass flow rate through film holes at $\pm 15^\circ$	U_∞	incident mainstream velocity at $X/b = 20$ for the no grid case
$\dot{m}_{40}$	mass flow rate through film holes at $\pm 40^\circ$	x	streamwise distance from stagnation (along test surface)
M	blowing ratio, $(\rho U)_s/(\rho U)_\infty$	X	streamwise distance from turbulence grid location
n	number of thermocouples in a row (spanwise direction) at any streamwise location	z	spanwise distance.
Nu_D	local Nusselt number based on leading edge diameter	Greek symbols	
$\overline{Nu}_D$	spanwise averaged Nusselt number	η	local film effectiveness
P	film hole pitch	$\bar{\eta}$	spanwise averaged film effectiveness
$\overline{q''}$	spanwise averaged forced convection heat flux with film injection	ν	kinematic viscosity
q''_{cond}	local conduction heat loss flux	ρ_s	injectant density
$q''_{cond,g}$	local conduction heat gain flux	ρ_∞	mainstream density
q''_{gen}	local generated surface heat flux	ϕ	overall cooling effectiveness.

injection; 4-d film injection provides lower heat flux ratio than 3-l film injection under higher mainstream turbulence conditions.

All the studies mentioned in the previous paragraph, [13–16], were carried out at the Reynolds number of 100 000. The Reynolds numbers for turbines operating at low mainstream velocities or for smaller turbines are much less than 100 000. Hence, it is very important to study the effect of Reynolds number on film cooling under high mainstream turbulence flow conditions.

This paper focuses on the effect of Reynolds number on leading edge heat transfer coefficient and film effectiveness with and without the turbulence grid for flow across a blunt body with a semi-cylinder leading edge and a flat afterbody. Representative results for two row film injection ($\pm 15^\circ$ and $\pm 40^\circ$) through 3-d and 4-d spaced film holes, at the Reynolds numbers of 40 000 and 25 000 are presented and compared with the previously published results at the Reynolds number of 100 000 from Mehendale and Han [13, 16]. Reynolds number effects for several other film hole configurations are also mentioned. The objectives of this study are: (a) to study the effect of Reynolds number on heat transfer coefficient and film effectiveness downstream of the film holes and (b) to determine which Reynolds number provides lower heat flux ratio.

TEST APPARATUS AND INSTRUMENTATION

The test apparatus was the same as used by Mehendale and Han [13, 16] and was designed as a suction type low speed, low turbulence wind tunnel. It consisted of a flow straightener, an inlet nozzle, a turbulence grid, and a test duct with the test section.

Both test models (3-d and 4-d spacing) were blunt bodies with semi-cylinder leading edges and flat afterbodies. They were made of wood. A schematic of the leading edge with two rows of 3-d spaced film holes is shown in Fig. 1. The leading edge diameter of 15.2 cm created a 20% flow blockage. Film holes were 1.1 cm in diameter and were spaced 3-d and 4-d apart for the two test models. The film holes were located at $\pm 15^\circ$ and $\pm 40^\circ$ and were inclined at 30° and 90° with the spanwise and streamwise directions, respectively, for both test models. One inlet port supplied the injectant to all film holes in the leading edge region.

Stainless steel foil strips, each 25 cm long × 3.8 cm wide × 0.005 cm thick, were cemented vertically on both test models. Holes were cut in the leading edge foils to match the film holes in the test models. The foils were separated by 0.8 mm gaps that were filled with silicone caulk and made flush with the foil surface. All foils were electrically connected in series by copper bus bars. A variac controlled the voltage across the foils. Thus, the test models provided an almost constant generated surface heat flux boundary condition (except for the foils with film holes) for the heat transfer coefficient tests; otherwise, it provided an almost adiabatic surface boundary condition for the film effectiveness tests.

Calibrated thirty-six gage copper–constantan thermocouples were cemented on the undersides of the foils in the leading edge region and in the flat-sidewall

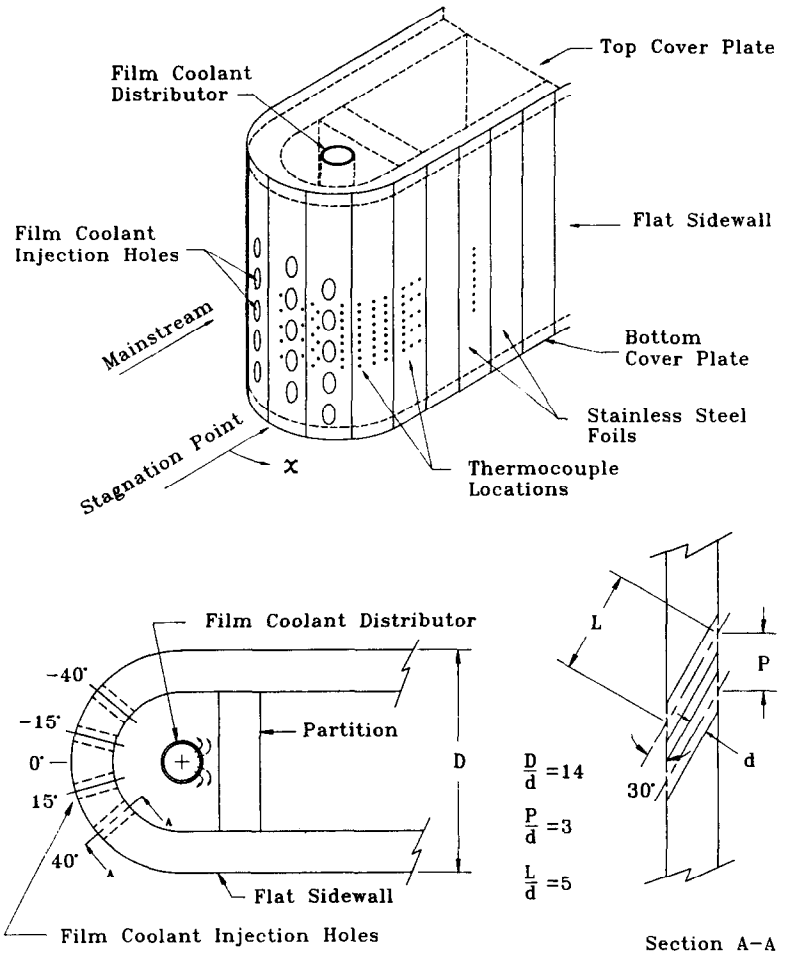

FIG. 1. Schematic of the leading edge with 3-d spaced holes.

region. Additional thermocouples were attached on the inner wall of the test model. Thermocouples were inserted in the bottommost film holes to measure the injectant temperature. All thermocouples were connected to a datalogger interfaced with a PC.

A calibrated hot wire (single wire) together with a constant temperature anemometer and a high speed digitizer was used to record fluctuating velocity data.

TEST CONDITIONS AND DATA ANALYSIS

Flow symmetry was established by checking the mainstream flow velocities, at corresponding locations on either side of the test model, to be equal. Tests were conducted at the Reynolds numbers ($Re_D = U_\infty D/\nu$) of 100000, 40000, and 25000. A nominal blowing ratio (based on the average injectant mass flux) of 0.8 was studied. Two upstream turbulence conditions—without the turbulence grid and with the turbulence grid—were studied. The streamwise turbulence intensities for the no grid and the turbulence grid cases at the three Reynolds numbers are given in Table 1.

The injectant centerline velocity at the exit of each film hole in a row was within $\pm 5\%$ for $\pm 15°$ rows and $\pm 4\%$ for $\pm 40°$ rows. The injectant flow turbulence intensity (the r.m.s. fluctuations in the injectant flow at the exit of each hole with the mainstream flow normalized by the incident mainstream velocity) was 7–12% at the blowing ratio of 0.8. The turbulence intensity at the exit of film holes in any row was fairly uniform. The $\dot{m}_{40°}/\dot{m}_{15°}$ ratio at the nominal blowing ratio of 0.8 was 1.5.

Heat transfer coefficient

Both injectant and mainstream were at ambient temperature and the wall temperature was maintained

Table 1.

No grid	With grid	Re_D
0.75%	9.67%	100000
0.73%	7.59%	40000
1.37%	8.53%	25000

25–30°C higher (based on location) than the mainstream temperature for all test cases.

As in Mehendale and Han [13, 16], the local heat transfer coefficient was calculated as

$$h = \frac{q''_{gen} - q''_{loss}}{T_w - T_\infty} = \frac{q''_{gen} - (q''_{cond} + q''_{rad})}{T_w - T_{aw}} \quad (1)$$

where T_w is the local wall temperature with foil heat and T_{aw} is the local adiabatic wall temperature (without foil heat).

Results from heat loss tests (Mehendale *et al.* [12] and Mehendale and Han [13]) were used to estimate the total heat loss in equation (1) above. Depending on the Reynolds number, the conduction and radiation heat losses were 3–8% and 10–25%, respectively, of the generated heat. Heat loss through the tiny thermocouple wires was estimated to be less than 0.1% and axial and lateral conduction through the thin foil was also found to be less than 0.1%.

The local Nusselt number was calculated from $Nu_D = hD/k$. The local Nusselt numbers at a given streamwise location were averaged to obtain the spanwise averaged Nusselt number ($\overline{Nu_D}$) at that location.

Film effectiveness

The injectant temperature was maintained about 25°C higher than the ambient mainstream temperature for all test cases.

As in Mehendale and Han [13, 16], the local film effectiveness was calculated as

$$\eta = \frac{T_w - T_\infty}{T_s - T_\infty} + \frac{(q''_{cond} + q''_{rad}) - q''_{cond,g}}{h(T_s - T_\infty)} \quad (2)$$

where T_w is the local wall temperature as a result of the mixing of the hotter injectant with the ambient mainstream, T_s is the hotter injectant temperature, and h is at corresponding test conditions.

The local film effectiveness values at a given streamwise location were averaged to obtain the spanwise averaged film effectiveness ($\bar{\eta}$) at that location.

Heat flux ratio

Since the objective of film injection is to reduce the heat flux (heat load) to a gas turbine component, heat loads for the film cooled model and for the no film holes model should be compared.

As in Mick and Mayle [11] and Mehendale and Han [13, 16], the spanwise averaged heat flux ratio was calculated as

$$\frac{\overline{q''}}{\overline{q''_0}} = \frac{1}{n}\sum_{i=1}^{n} \frac{h(x,z_i)}{h_0(x,z_i)}\left(1 - \frac{\eta(x,z_i)}{\phi}\right) \quad (3)$$

where $\phi = (T_w - T_\infty)/(T_s - T_\infty)$ is overall cooling effectiveness. For gas turbine blades, ϕ usually ranges from 0.5 to 0.7. A typical value of 0.6 was chosen for ϕ. This is very close to the value of ϕ for our test conditions. Local heat transfer coefficients for the test model without film holes were used from Mehendale *et al.* [12]. It should be noted that a heat flux ratio of less than unity indicates that film injection reduces surface heat load over the no film holes case.

It should also be noted that for $\phi = 0.6$, the film effectiveness has 1.67 times more weight than heat transfer coefficient and hence, the film effectiveness values play a more dominant role in determining the heat flux ratio.

An uncertainty analysis as in Kline and McClintock [17] showed that based on 20:1 odds, the uncertainty in heat transfer coefficient and film effectiveness values around the film holes is ±15% and downstream of the film holes is ±5%.

RESULTS AND DISCUSSION

Flow conditions

The local streamwise velocity and turbulence intensity distributions along centerline and right-side line for both the no grid and the turbulence grid conditions are shown in Mehendale *et al.* [12]. The centerline turbulence intensity decreases first with increasing distance from the turbulence grid; but as stagnation is approached, there is an increase in turbulence intensity due to a decrease in the local average mainstream velocity. For a given upstream condition, the minimum value of the corresponding centerline turbulence intensity curve (about $0.65D$ upstream of the leading edge) was chosen as the reference turbulence intensity for that condition. The reference turbulence intensities for the no grid and turbulence grid at the three Reynolds numbers are given in Table 1.

Heat transfer coefficient

The spanwise averaged heat transfer coefficient distributions for the test model without film holes for the two upstream turbulence conditions are shown in Fig. 2. With increasing distance from stagnation, boundary layer growth causes a decrease in heat transfer coefficients in the leading edge region for all test cases. Bellows and Mayle [18] measured detailed velocity profiles in the region where the semi-cylinder leading edge merges with the flat afterbody and found the existence of a separation bubble. As discussed in Mick and Mayle [11] and Mehendale *et al.* [12], the decrease

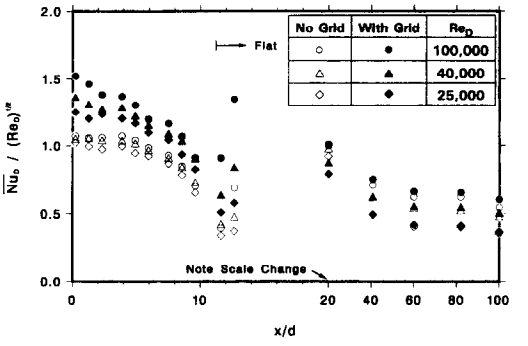

FIG. 2. Effect of Reynolds number on $\overline{Nu_D}/(Re_D)^{0.5}$ for a test model without film holes, with and without turbulence grid.

and rapid increase in heat transfer coefficient around $x/d = 12$ is due to separation of the leading edge laminar boundary layer and subsequent turbulent reattachment, respectively. On the flat sidewall, the heat transfer coefficients for all test cases decrease monotonically due to boundary layer growth.

For the no turbulence grid case, leading edge heat transfer coefficients for all three Reynolds numbers are within $\pm 5\%$ of each other. This is evidenced by the standard correlation for laminar stagnation flow, $St = 0.57Pr^{-0.6}Re^{-0.5}$, which implies that $Nu/Re^{0.5}$ is independent of Reynolds number. Downstream of turbulent reattachment ($x/d > 13$), the effect of Reynolds number is more significant. This is evidenced by the standard correlation for turbulent flow on a flat plate, $St = 0.0307Pr^{-0.4}Re^{-0.2}$, which implies that $Nu/Re^{0.5} \propto Re^{0.3}$. For the turbulence grid case, the boundary layer in the leading edge region is a highly disturbed laminar boundary layer and the heat transfer coefficient behavior may be characterized by $Nu/Re^{0.5} \propto Re^{m}$ where 0(laminar) $< m <$ 0.3(fully turbulent). Similar to the no turbulence grid case, a decrease in heat transfer coefficients in the leading edge region due to boundary layer growth is observed. The turbulence grid generated mainstream flow fluctuations considerably enhance the heat transfer coefficients in the leading edge region. The mainstream turbulence induced increases in heat transfer coefficients on the flat sidewall are not as significant as on the leading edge due to decay of turbulence. At these high mainstream turbulence levels, an increase in Reynolds number causes an increase in heat transfer coefficient. This is apparent from Fig. 2 where the heat transfer coefficients for $Re_D = 40\,000$, in spite of lower streamwise turbulence intensity, are higher than for $Re_D = 25\,000$ over the entire test surface.

The effect of Reynolds number on spanwise averaged heat transfer coefficients without the turbulence grid, at the intermediate blowing ratio of 0.8 through two rows of film holes spaced 3-d apart, is shown in Fig. 3. Peaks are evident just downstream of the film hole row locations. This is because the strong interaction between the injectant jet and the mainstream disturbs the boundary layer and results in higher heat transfer coefficients. Further downstream of the film holes, boundary layer stabilization and growth cause a reduction in heat transfer coefficients. Even though the momentum flux ratio for a given blowing ratio remains the same for all three Reynolds numbers (i.e. the jet penetration should be the same), differences in the boundary layer velocity profiles for the three Reynolds numbers cause different jet penetrations. The momentum near the surface is higher for the higher Reynolds number. This causes more jet deflection and results in higher heat transfer coefficients downstream of the film holes for higher Reynolds numbers. Far downstream of the leading edge film holes, the effect of Reynolds number on the flat sidewall is similar to the no film holes test model.

The effect of Reynolds number on spanwise averaged heat transfer coefficients with the turbulence grid, at the intermediate blowing ratio of 0.8 through two rows of film holes spaced 3-d apart, is shown in Fig. 4. As for the case of no turbulence grid, an increase in Reynolds number causes an increase in heat transfer coefficients over the entire test surface. An increase in the levels of heat transfer coefficients are seen over the previous figure due to high mainstream turbulence. For the Reynolds numbers of 40 000 and 25 000, the changes from the no grid to the turbulence grid are very small since the boundary layer is thicker and the mainstream turbulence is unable to penetrate the thicker boundary layer. The effect of mainstream turbulence on heat transfer coefficients is more significant for the Reynolds number of 100 000. This is because the boundary layer at this Reynolds number is much thinner and the mainstream flow fluctuations can easily penetrate the boundary layer. As turbulence decays with distance, the effect of mainstream turbulence is less prominent on the flat sidewall.

The effect of Reynolds number on spanwise averaged heat transfer coefficients with the turbulence grid, at the intermediate blowing ratio of 0.8 through two rows of film holes spaced 4-d apart, is shown in Fig. 5. As for the case of 3-d film injection, an increase in Reynolds number causes an increase in heat transfer coefficients over the entire test surface. Since the

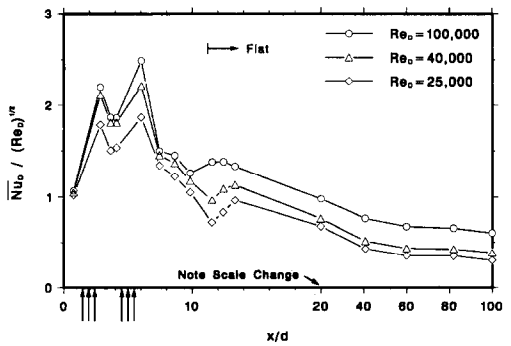

FIG. 3. Effect of Reynolds number on $\overline{Nu_D}/(Re_D)^{0.5}$ at $M = 0.8$ (3-d spacing) and without turbulence grid.

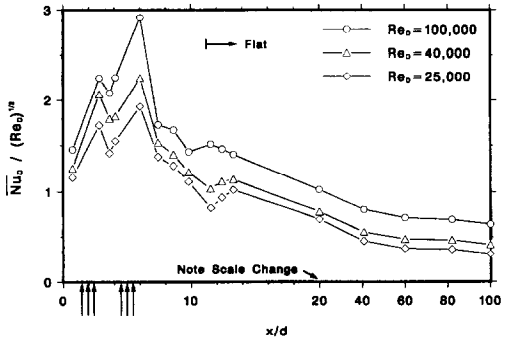

FIG. 4. Effect of Reynolds number on $\overline{Nu_D}/(Re_D)^{0.5}$ at $M = 0.8$ (3-d spacing) and with turbulence grid.

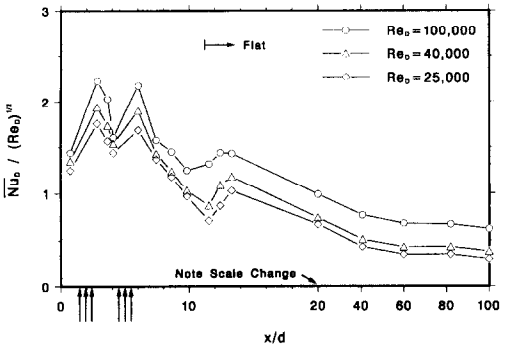

FIG. 5. Effect of Reynolds number on $\overline{Nu_D}/(Re_D)^{0.5}$ at $M = 0.8$ (4-d spacing) and with turbulence grid.

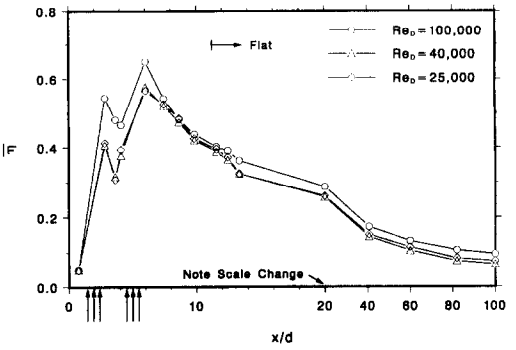

FIG. 7. Effect of Reynolds number on $\bar{\eta}$ at $M = 0.8$ (3-d spacing) and with turbulence grid.

film holes are spaced farther apart, the injectant jet disturbed boundary layer effect is not as strong at all spanwise locations and hence the heat transfer coefficients are less than the 3-d case. This film hole spacing effect is more prominent for the Reynolds number of 100 000.

Film effectiveness

The effect of Reynolds number on spanwise averaged film effectiveness without the turbulence grid, at the intermediate blowing ratio of 0.8 through two rows of film holes spaced 3-d apart, is shown in Fig. 6. Peaks are evident just downstream of the film hole row locations due to better film coverage from an undiluted injectant jet. Further downstream of the film holes, injectant dilution (mixing with mainstream) causes a reduction in film effectiveness. In general, an increase in Reynolds number causes an increase in film effectiveness over most of the test surface. This is because, even though the momentum flux ratio for a given blowing ratio remains the same for all three Reynolds numbers (i.e. the jet penetration should be the same), differences in boundary layer velocity profiles for the three Reynolds numbers cause different penetrations. Higher Reynolds number flow has higher momentum near the surface. This causes more jet deflection and jet entrapment within the boundary layer and results in higher film effectiveness downstream of the film holes at higher Reynolds numbers. Since the mass flow rate of the injectant increases with the Reynolds number, higher film effectiveness values are seen on the flat sidewall.

The effect of Reynolds number on spanwise averaged film effectiveness with the turbulence grid, at the intermediate blowing ratio of 0.8 through two rows of film holes spaced 3-d apart, is shown in Fig. 7. As for the no turbulence grid case, an increase in Reynolds number causes an increase in film effectiveness over most of the test surface. For the Reynolds numbers of 40 000 and 25 000, the changes in film effectiveness from the no grid to the turbulence grid are very small indicating that the boundary layer is thicker and the mainstream turbulence cannot penetrate the boundary layer. The effect of mainstream turbulence on film effectiveness just downstream of the film holes for the Reynolds number of 100 000 may be due to more mixing. The effect of mainstream turbulence is less prominent on the flat sidewall.

The effect of Reynolds number on spanwise averaged film effectiveness with the turbulence grid, at the intermediate blowing ratio of 0.8 through two rows of film holes spaced 4-d apart, is shown in Fig. 8. As for the case of 3-d spaced two row film injection with turbulence grid, an increase in Reynolds number causes an increase in film effectiveness over the entire test surface; however, the effect of Reynolds number is more distinct than in the 3-d spacing case. Since the film holes are spaced farther apart, the film coverage

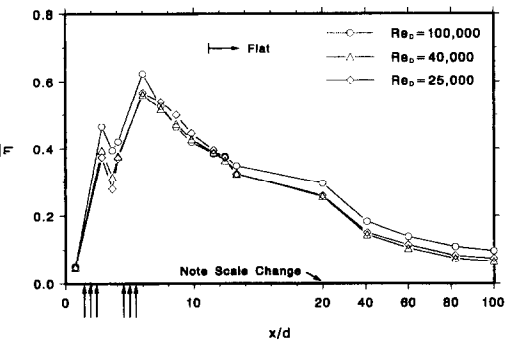

FIG. 6. Effect of Reynolds number on $\bar{\eta}$ at $M = 0.8$ (3-d spacing) and without turbulence grid.

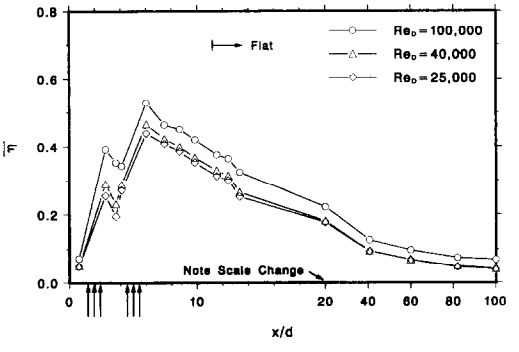

FIG. 8. Effect of Reynolds number on $\bar{\eta}$ at $M = 0.8$ (4-d spacing) and with turbulence grid.

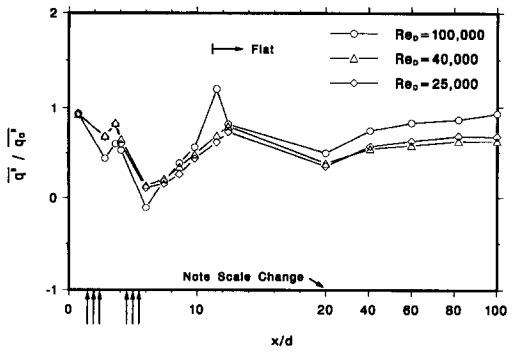

FIG. 9. Effect of Reynolds number on $\overline{q''}/\overline{q_0''}$ at $M = 0.8$ (3-d spacing) and without turbulence grid.

is not as good at all spanwise locations and hence, film effectiveness is less than the 3-d spacing case.

Heat flux ratio

The effect of Reynolds number on spanwise averaged heat flux (heat load) ratio without the turbulence grid, at the intermediate blowing ratio of 0.8 through two rows of film holes spaced 3-d apart, is shown in Fig. 9. It should be noted that film injection is counterproductive if the heat load ratio is greater than unity. Heat load ratios over most of the test surface, except in the region where the leading edge merges with the flat sidewall, are much less than unity indicating a considerable reduction in heat flux over the no film holes test model. This indicates that a substantial reduction in heat transfer is achieved by film injection. Heat load ratios just downstream of the film holes are the lowest at the Reynolds number of 100 000, because the Reynolds number of 100 000 provides the highest film effectiveness just downstream of the film holes. The Reynolds numbers of 40 000 and 25 000 produce similar values over most of the leading edge. On the flat sidewall, the Reynolds number of 100 000 produces higher heat load ratios due to smaller film effectiveness and higher heat transfer coefficient values.

The effect of Reynolds number on spanwise averaged heat load ratio with the turbulence grid, at the intermediate blowing ratio of 0.8 through two rows of film holes spaced 3-d apart, is shown in Fig. 10. Similar to the no turbulence grid case, the Reynolds number of 100 000 provides the lowest heat flux ratios in the leading edge region; whereas, it produces the highest heat flux ratios in the flat sidewall region. Similar heat load ratios are observed for the Reynolds numbers of 40 000 and 25 000 over most of the test surface. The heat load ratios for all three Reynolds numbers at all locations are less than unity indicating reduced heat transfer over the no film holes test model. A decrease in the levels of the heat load ratios are seen over the previous figure. This is because the denominator in equation (3) is now the heat transfer coefficient from the no film holes 'with turbulence grid' case, which is higher than the heat transfer coefficient from the no film holes 'no grid' case used for the previous figure.

The effect of Reynolds number on spanwise averaged heat load ratio with the turbulence grid, at the intermediate blowing ratio of 0.8 through two rows of film holes spaced 4-d apart, is shown in Fig. 11. As Reynolds number increases, the heat flux ratios reduce over the entire leading edge. The Reynolds number of 100 000 produces the highest heat flux ratio in the flat sidewall region. The heat load ratios for all three Reynolds numbers at all locations are less than unity indicating reduced heat transfer over the no film holes test model. The heat load ratios for the 3-d spacing are lower than the 4-d spacing, because the film effectiveness values for the 3-d spacing are higher than the 4-d spacing.

Note

Data were also obtained at the blowing ratios of 0.4 and 1.2 (in addition to the blowing ratio of 0.8 presented in this paper) for two rows of film holes spaced 3-d and 4-d apart. The Reynolds number effect is similar to that discussed above for the blowing ratio of 0.8. Apart from film injection through two rows of film holes, data were also obtained at the blowing ratios of 0.4, 0.8, and 1.2 at several mainstream turbulence conditions for the following film hole geometries—a single row of film holes at $\pm 15°$ spaced 3-d apart, a single row of film holes at $\pm 40°$ spaced 3-d apart, two rows of film slots spaced 3-l apart, a single row of film slots at $\pm 15°$ spaced 3-l apart, and a single row of film slots at $\pm 40°$ spaced 3-l apart. Since the

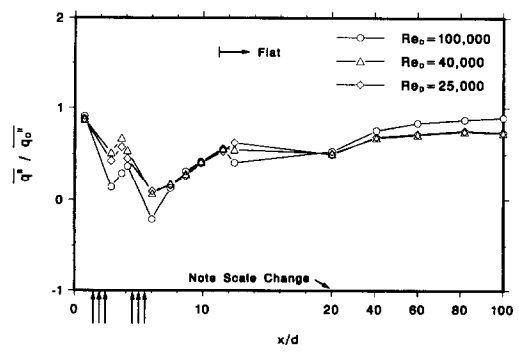

FIG. 10. Effect of Reynolds number on $\overline{q''}/\overline{q_0''}$ at $M = 0.8$ (3-d spacing) and with turbulence grid.

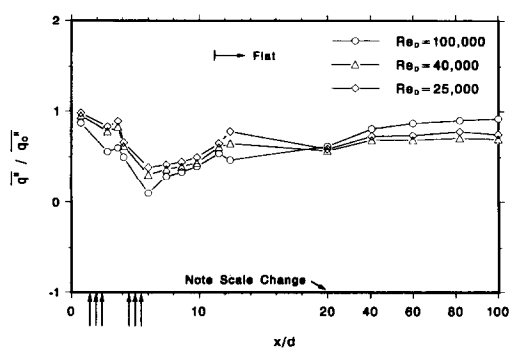

FIG. 11. Effect of Reynolds number on $\overline{q''}/\overline{q_0''}$ at $M = 0.8$ (4-d spacing) and with turbulence grid.

Reynolds number effect is similar for all these test cases, data for these test cases are not repeated in this paper due to space limitations.

CONCLUDING REMARKS

The effect of mainstream Reynolds number under elevated mainstream turbulence conditions on heat transfer coefficient, film effectiveness and heat flux of the leading edge test model was investigated. Tests were performed at the Reynolds numbers of 100 000, 40 000, and 25 000 for without turbulence grid and with turbulence grid cases. The main findings are:

1. In general, an increase in Reynolds number causes an increase in heat transfer coefficients with film injection over most of the test surface for all injection geometries, at all blowing ratios, and at all turbulence levels studied. This increase is due to the flow momentum near the wall being higher at a higher Reynolds number.
2. The effect of mainstream turbulence on heat transfer coefficients with film injection is more prominent at the Reynolds number of 100 000 because of disturbance penetration through a thinner boundary layer. Mainstream turbulence does not seem to affect the heat transfer coefficients at the lower Reynolds numbers of 40 000 and 25 000 because of thicker boundary layers.
3. In general, an increase in Reynolds number causes an increase in film effectiveness downstream of the film holes for all injection geometries, at all blowing ratios, and at all turbulence levels studied. This increase is due to the flow momentum near the wall being higher at higher Reynolds number thus causing more injectant jet deflection and entrapment.
4. In general, mainstream turbulence does not seem to affect the film effectiveness distributions at the lower Reynolds numbers of 40 000 and 25 000 because of a thicker boundary layer.
5. In general, lower heat flux (load) ratios are achieved at higher Reynolds number in the leading edge region for all injection geometries, at all blowing ratios, and at all turbulence levels studied. This is because the film effectiveness at higher Reynolds number is higher. In general, the effect of Reynolds number is reversed on the flat sidewall where higher Reynolds number produces significantly higher heat transfer coefficients. In general, heat flux (load) ratios at all locations for all test cases are lower than unity indicating lower heat transfer over the no film holes test model.

Acknowledgement—The project was sponsored by Textron-Lycoming Division through contract # *H*164150. Their support is greatly appreciated.

REFERENCES

1. R. J. Goldstein, E. R. G. Eckert and J. W. Ramsey, Film cooling with injection through holes: adiabatic wall temperatures downstream of a circular hole, *ASME J. Engng Power* **90,** 384–395 (1968).
2. R. J. Goldstein, E. R. G. Eckert, V. L. Eriksen and J. W. Ramsey, Film cooling following injection through inclined circular tubes, *Israel J. Technol.* **8,** 145–154 (1970).
3. V. L. Eriksen and R. J. Goldstein, Heat transfer and film cooling following injection through inclined circular tubes, *ASME J. Heat Transfer* **96,** 239–245 (1974).
4. J. F. Muska, R. W. Fish and M. Suo, The additive nature of film cooling from rows of holes, *ASME J. Engng Power* **98,** 457–464 (1976).
5. M. Sasaki, K. Takahara, K. Sakata and T. Kumagai, Study on film cooling of turbine blades, *Bulletin of the JSME* **19**(137), 1344–1352 (1976).
6. G. Bergeles, A. D. Gosman and B. E. Launder, Near-field character of a jet discharged through a wall at 30° to a mainstream, *AIAA J.* **15,** 499–504 (1977).
7. R. E. Mayle, F. C. Kopper, M. F. Blair and D. A. Bailey, Effect of streamline curvature on film cooling, *ASME J. Engng Power* **99,** 77–82 (1977).
8. M. Y. Jabbari and R. J. Goldstein, Adiabatic wall temperature and heat transfer downstream of injection through two rows holes, *ASME J. Engng Power* **100,** 303–307 (1978).
9. J. C. Han and A. B. Mehendale, Flat plate film cooling with steam injection through one row and two rows of inclined holes, *ASME J. Turbomach.* **108,** 137–144 (1986).
10. B. Schönung and W. Rodi, Prediction of film cooling by a row of holes with a two dimensional procedure, *ASME J. Turbomach.* **109,** 579–587 (1987).
11. W. J. Mick and R. E. Mayle, Stagnation film cooling and heat transfer, including its effect within the hole pattern, *ASME J. Turbomach.* **110,** 66–72 (1988).
12. A. B. Mehendale, J. C. Han and S. Ou, Influence of high mainstream turbulence on leading edge heat transfer, *ASME J. Heat Transfer* **113,** 843–850 (1991).
13. A. B. Mehendale and J. C. Han, Influence of high mainstream turbulence on leading edge film cooling heat transfer, *ASME J. Turbomach.* **114,** 707–715 (1992).
14. S. Ou, A. B. Mehendale and J. C. Han, Influence of high mainstream turbulence on leading edge film cooling heat transfer: effect of film hole row location, *ASME J. Turbomach.* **114,** 716–723 (1992).
15. S. Ou and J. C. Han, Influence of mainstream turbulence on leading edge film cooling heat transfer through two rows of inclined film slots, *ASME J. Turbomach.* **114,** 724–733 (1992).
16. A. B. Mehendale and J. C. Han, Influence of high mainstream turbulence on leading edge film cooling heat transfer: effect of film hole spacing, *Int. J. Heat Mass Transfer* **35,** 2593–2604 (1992).
17. S. J. Kline and F. A. McClintock, Describing uncertainties in single-sample experiments, *Mech. Engng* **75,** 3–8 (1953).
18. W. J. Bellows and R. E. Mayle, Heat transfer downstream of a leading edge separation bubble, *ASME J. Turbomach.* **108,** 131–136 (1986).